EE

BNL-52439
FORMAL REPORT
UC-414

CRYSTALLINE BEAMS

JIE WEI,
XIAO-PING LI (BIOSYM Technologies, Inc.) and ANDREW M. SESSLER (LBL)

OCTOBER 6, 1994

RHIC PROJECT

Brookhaven National Laboratory
Associated Universities, Inc.
Upton, NY 11973-5000

Under Contract No. DE-AC02-76CH00016 with the

UNITED STATES DEPARTMENT OF ENERGY

BNL-52439
FORMAL REPORT
UC-414

CRYSTALLINE BEAMS

JIE WEI,
XIAO-PING LI (BIOSYM Technologies, Inc.) and ANDREW M. SESSLER (LBL)

OCTOBER 6, 1994

RHIC PROJECT

Brookhaven National Laboratory
Associated Universities, Inc.
Upton, NY 11973-5000

Under Contract No. DE-AC02-76CH00016 with the

UNITED STATES DEPARTMENT OF ENERGY

DISCLAIMER

Printed in the United States of America
Available from
National Technical Information Service
U.S. Department of Commerce
5285 Port Royal Road
Springfield, VA 22161

NTIS price codes:
Printed Copy: A06; Microfiche Copy: A01

Crystalline Beams *

Jie Wei
Brookhaven National Laboratory, Upton, New York 11973
Xiao-Ping Li
BIOSYM Technologies Inc., 9685 Scranton Rd., San Diego, CA 92121
Andrew M. Sessler
Lawrence Berkeley Laboratory, 1 Cyclotron Road, Berkeley, California 94720

Abstract

The low energy states of a beam of charged particles subject to circumferentially varying guiding and focusing forces are studied by first deriving a Hamiltonian in the rest frame of the circulating reference particle and then using the molecular dynamics method. In an alternating gradient structure, operating below the transition energy, (but not in a constant gradient ring), the lowest state is ordered. The nature of the ground state depends upon the beam density and the ring parameters. At very low temperature the crystal remains intact for a long time, but as temperature increases it rapidly gains energy from the lattice. In order for the crystalline beam to last a meaningful length of time, the storage ring should be designed such that the lattice periodicity of the machine is at least twice as high as the betatron frequencies.

1. INTRODUCTION

The ground states of crystalline beams were first studied, in seminal work,[1] – [3] by Schiffer and his colleagues. Their work assumed a storage ring model in which charged particles are subject to time-independent[4] – [11] harmonic forces in both transverse directions. Subsequently, many authors studied crystallization in a time-dependent focusing potential which replicated some of the features of alternating gradient (AG) focusing, and with time-dependent shear which replicated some of the features of the alternate bending and straight sections of a storage ring.[12] – [15] Nevertheless, questions remain for many years about whether or not an ordered state can be created in a real storage ring. Furthermore, with laser cooling very low (longitudinal) temperatures of stored beams have recently been achieved.[16] – [17] Thus it became prudent to develop the tools which will allow one to make calculations that incorporate the characteristics of actual storage rings.

*Work performed under the auspice of the U.S. Department of Energy, supported by NSF Grant DMR-91-15342, and by the DOE, Office of Energy Research, Office of High Energy and Nuclear Physics, under Contract No.DE-AC03-76SF00098.

Recently, we have developed such a formalism and employ it to study the nature of the ordered state in actual storage rings.[18] We find that in operation below the transition energy, $\gamma < \gamma_t$, alternating gradient (AG) rings, as contrasted with constant gradient rings, can have a crystalline lowest energy–or ground state. This state will change periodically in time, "breathing" as the particles go around the storage ring, and is subject to periodic bending, straight sections, focusing lenses, and defocusing lenses. Under some conditions the changes are dramatic, the crystal periodically changing its shape and orientation, but the crystal remains for a very long time in the ground state; i.e., by this process very little heat is put into the crystal (possibly zero at zero temperature). In order to achieve the ordered state the beam must be very cold. We give results, in typical machine parameters, for just how cold (expressed in terms of energy spread and emittance) must be the beam. We show that there exists a temperature above which the crystal rapidly melts.

This paper summarizes the results of our recent studies on crystalline beams.[18] – [22] In order to employ molecular dynamics (MD) method, commonly used in condensed matter physics for quantitative studies, we first derive in Section 2 the equations of motion for the particles in the rotating rest frame of the reference particle. We include in the formalism that the particles are confined by the external guiding and focusing magnetic fields, and that they are confined in a conducting vacuum pipe while interacting with each other via the Coulomb force. In Section 3, we derive the conditions for crystallization in a circular storage ring. After describing the MD method and models for the calculation in Section 4, we present in Section 5 the numerical results on the crystalline-beam ground-state structure, and discuss in Sections 6 and 7 the mechanism for heat transfer, melting and break-up. Finally, the conclusions and a discussion are given in section 8.

2. EQUATIONS OF MOTION IN ROTATING BEAM FRAME

In order to adopt the molecular dynamics methods we must be in the frame of reference of the particles, i.e., a rotating frame (x, y, z, t) of a reference particle in which the orientation of the axes is rotating so that the axes are constantly aligned to the radial (x), vertical (y), and tangential (z) direction of motion. This is, of course, an accelerating frame of reference. We can derive the equations in the laboratory frame and then transform to the moving frame, but it is most convenient to derive the equations directly in the beam frame, employing the formalism of general relativity.[23] One may think of the result of this process as finding the relativistic generalization of centrifugal and Coriolis forces. In the frame of the reference particle, the particle motion is non-relativistic. The MD method can thus be directly adopted. The rather lengthy derivation was given in a Laboratory Report[18] and summarized in a Conference Proceeding Publication:[19] here we only summarize the procedure and present the results.

First, we express the equations of motion of a charged particle in a general tensor formalism applicable to any arbitrary coordinate system. The Lorentz force experi-

enced by the particle is constructed as a product of the electromagnetic (EM) field tensor and the four-velocity. Starting from the laboratory frame, the EM field tensor is written by means of the components of the electric and magnetic fields. Then, tensor algebra is used to transform this field tensor into the rest frame of the reference particle. With a similar transformation, the metric tensor of the beam rest frame can be obtained. The equations of motion can thus be constructed in the rest frame, from which both centrifugal and Coriolis forces can easily be identified. Finally, these equations are scaled in terms of dimensionless quantities for the convenience of computer simulation and analysis.

It is convenient to scale dimensions in terms of ξ, with $\xi^3 = r_0\rho^2/\beta^2\gamma^2$, where r_0 is the classical particle radius (Z^2e^2/m_0c^2), Ze is the electric charge, the velocity of a reference particle is βc, its energy is $\gamma m_0 c^2$, and it moves on an orbit with bending radius ρ in magnetic field B_0. We measure time in units of $\rho/\beta\gamma c$ and energy in units of $\beta^2\gamma^2 Z^2e^2/\xi$. In a bending region, with magnetic field B_0, we have derived the equations of motion

$$\begin{cases} \ddot{x} - \gamma\dot{z} + (-\gamma^2 + 1)x = -\dfrac{\partial V_C}{\partial x}, \\ \ddot{y} = -\dfrac{\partial V_C}{\partial y}, \\ \ddot{z} + \gamma\dot{x} = -\dfrac{\partial V_C}{\partial z}. \end{cases} \tag{1}$$

Here, the dots denote differentiations with respect to the time t measured in the above units, the Coulomb potential is

$$V_C(x,y,z) = \sum_j \frac{1}{\sqrt{(x_j - x)^2 + (y_j - y)^2 + (z_j - z)^2}}, \tag{2}$$

and the summation, j, is over all the other particles. The Hamiltonian that corresponds to Eq. 2 is

$$H(x, P_x, y, P_y, z, P_z; t) = \frac{1}{2}\left(P_x^2 + P_y^2 + P_z^2\right) - \gamma x P_z + \frac{1}{2}x^2 + V_C(x,y,z). \tag{3}$$

In a straight section, where there is no bending of particles, there often are focusing magnets. If focusing is supplied by a quadrupole of field gradient B_1 so that $B_x = B_1 y$ and $B_y = B_1 x$, and the focusing strength is characterized by $n = -B_1\rho/B_0$, the equations of motion are

$$\begin{cases} \ddot{x} - nx = -\dfrac{\partial V_C}{\partial x}, \\ \ddot{y} + ny = -\dfrac{\partial V_C}{\partial y}, \\ \ddot{z} = -\dfrac{\partial V_C}{\partial z}. \end{cases} \tag{4}$$

The corresponding Hamiltonian is

$$H(x, P_x, y, P_y, z, P_z; t) = \frac{1}{2}\left(P_x^2 + P_y^2 + P_z^2\right) + \frac{n}{2}(-x^2 + y^2) + V_C(x, y, z). \quad (5)$$

As the particle goes around the storage ring, the appropriate equations of motion must be employed. The change from those corresponding to a curved section to those corresponding to a straight section incorporates, in a quantitatively correct manner, the effect of shear (given by the term $\gamma x P_z$ in the Hamiltonian Eq. 3). Similarly, the effect of alternate gradient is incorporated, quantitatively correctly, by changing the field gradient n (positive for vertical focusing, negative for vertical defocusing, and zero for an open straight section). In the reduced units, the revolution period of the reference particle in the storage ring is $2\pi R/\rho$, where $2\pi R$ is the circumference of the storage ring.

3. CONDITIONS FOR CRYSTALLIZATION

Consider a cyclotron magnet, i.e., a magnet that gives constant bending and constant focusing. The Hamiltonian in this case is

$$H(x, P_x, y, P_y, z, P_z; t) = \frac{1}{2}\left(P_x^2 + P_y^2 + P_z^2\right) - \gamma x P_z + \frac{1}{2}\left[(1-n)x^2 + ny^2\right] + V_C(x, y, z). \quad (6)$$

If the gradient of the magnet is such that n lies between zero and one, then the magnet, in combination with the centrifugal force, gives focusing in both the vertical and horizontal planes. Just the kind of storage rings, one would think, for the formation of a crystal and, yet, that is not true at all. The Hamiltonian in Eq. 6 is bounded from below only if $0 < n < 1 - \gamma^2$ (a proof is given in the Appendix). Since $\gamma > 1$, we see that this condition can never be satisfied and, as a result, crystalline beams can never exist in this case. In fact, the centrifugal force becomes defocusing when the particles are crystallized. Therefore, a weak-focusing machine consisting of a cyclotron magnet can not be used for crystallization.

On the other hand, an AG-focusing machine, in contrast to a weak-focusing machine, can be used for beam crystallization under appropriate conditions. Consider an AG machine of constant bending. The Hamiltonian is the same as in Eq. 6 but with n time-dependent. Assuming there is horizontal and vertical focusing, i.e. $\nu_x > 0$ and $\nu_y > 0$, where ν_x and ν_y are the horizontal and vertical tunes, it is easy to see that the Hamiltonian, in smooth approximation, is bounded from below if and only if $\gamma < \nu_x$ and, therefore, crystalline beams exist only if the ring is operated below the transition energy (a proof is given in the Appendix).

4. MOLECULAR DYNAMICS

In general, when Coulomb interactions and AG focusing are present it is impossible to solve the equations analytically; we obtain numerical solutions using molecular

dynamics. This method allows us to determine the lowest energy state in realistic storage rings (i.e., the actual ring lattice can be inserted in the computation) and, also, allows us to study behavior as the crystal temperature is increased from absolute zero. We can determine the temperature at which such a crystal melts; i.e., loses its long-range order as the particles go into a state in which they pass each other (as in a usual storage ring).

In the MD calculations we choose time and space steps, the number of particles in a MD super-cell, and the length of super-cells, so that the results are independent of these choices. Initially the positions and momenta of the particles are randomly chosen. In finding the ground state we "cool" once per lattice period by simply imposing a condition of periodicity (by averaging initial and final coordinates and momenta) while correcting P_z according to the amount of slippage in z for each particle and for many periods (typically 1000) and then turning the cooling off and observing no change (in one case for up to 10^6 lattice periods). The results are independent of initial conditions. We have checked that "cooling" which better replicates the actual experiments leads to the same state (but takes very long when the density is high).

Since Coulomb interaction is long ranged, an Ewald-type summation has to be performed to calculate the energy and the forces.[24] – [25] To simulate a real accelerator, we consider a bunch of charged particles confined in a perfectly conducting, infinitely long pipe. The periodic boundary condition is used only in the z direction, where the super-cell of length L (in unit of ξ) repeats itself to infinity. The energy due to two particles at $\mathbf{x}_i$ and $\mathbf{x}_j$, after all the image charges and equivalents in other super-cells are included, is

$$\phi(\mathbf{x}_i, \mathbf{x}_j) = \frac{1}{r_{ij}} + \frac{4}{L}\int_0^\infty \frac{\cosh(2z_{ij}k/L)J_0(2\rho_{ij}k/L) - 1}{\exp(2k) - 1}dk + \frac{2}{L}[\log(\pi b/L) + C] \quad (7)$$

where $z_{ij} = z_i - z_j$, $\rho_{ij} = [(x_i - x_j)^2 + (y_i - y_j)^2]^{1/2}$, $r_{ij} = (z_{ij}^2 + \rho_{ij}^2)^{1/2}$, b is the radius of the pipe, and C is the Euler constant. The condition $\rho_{ij} << b$ is used and z_{ij} is understood to be between $-L/2$ and $L/2$ (if z_{ij} falls outside this range, an integer times of L is added to it to bring it to the correct range). The equations of motion is integrated by the 4th order Runge-Kutta method. The integration in Eq. 7 is usually performed by a 15th order Gauss-Laguerre method, except for particles of small distance $\rho_{ij}/L \ll 1$ where polynomial approximations[26] can be used with sufficient accuracy to reduce the computation time.

5. GROUND-STATE STRUCTURES

When the condition for crystallization ($\gamma < \gamma_t$) is satisfied, crystalline beams of various densities can be formed. Let us now, for pedagogical purposes, separate the effect of "shear" from that of time-dependent focusing. We shall study, as we did in our earlier work,[18] – [20] an AG ring with a constant bending field. For a given ring, the nature of the ground state (which term is used to describe the periodic lowest energy state) depends upon the density of particles. When the density is low the ground state is a one-dimensional (1-D) chain. If the density is larger then the ground

state is a 2-D state that lies in the plane of weaker focusing, which is determined by whether $\nu_x^2 - \gamma^2$ is greater, or smaller, than ν_y^2. Notice that the focusing in a crystal is not determined simply by ν_x and ν_y, but by the factors $(\nu_x^2 - \gamma^2)^{1/2}$ and ν_y.

The (line) density at which a 1-D structure changes into a 2-D structure can be determined analytically. It is given by

$$\Delta_z^{-1} > 0.62 \left[\min(\nu_y^2, \nu_x^2 - \gamma^2)\right]^{1/3}, \tag{8}$$

where Δ_z is the nearest neighbor distance in z (given trivially in terms of the number of particles stored, the circumference of the storage ring, and γ). Notice that, in practice, one can change the focusing of a storage ring ("changing the operating point") and also change the storage energy. Thus the focusing can be readily changed and the effect of such change easily studied.

In an AG ring the 2-D crystal structure, as contrasted with the 1-D structure, will "breath" as the particles go about the storage ring. Despite this motion little energy is pumped into the crystal; it remains in its ground state for a very long time. Such behavior is not unexpected, for as particles go around AG storage rings the amplitude of their oscillation changes (β-function variation), and particles of different energy move closer or further apart (η-function variation), yet particles can be stored forever.[20] – [22]

We find, numerically, that when the line density is higher than that appropriate to a 2-D crystal, the particles arrange themselves into 3-D crystals; becoming helices and then helices within helices. An example is shown in Fig. 1. These structures are similar to, but differ in detail, from that given in Ref. 1. It is seen that the ratio between the average horizontal and vertical particle spacing is about $[\nu_y^2/(\nu_x^2 - \gamma^2)]^{1/3}$. When the horizontal and the vertical focusing strengths are about the same, $\nu_x^2 - \gamma^2 \approx \nu_y^2$, the interparticle spacing in these structures is approximately the same, and given (roughly) by the interparticle spacing when transition is made from a 1-D crystal to a 2-D crystal; i.e., can be characterized by ξ, ν_x^2, ν_y^2, and γ. Thus the crystal forms cylindrical shells within cylindrical shells, upon which the particles are deployed in such a way that the interparticle spacing is about the same. This behavior is very similar to that which occurs in ordinary crystals. It appears to be the case that a crystal forms no matter how high is the particle line density. Thus one obtains that the maximum spatial density, λ_{max}, for a crystal of high line density in the laboratory frame is

$$\lambda_{max} \approx \frac{\gamma \nu_y \sqrt{\nu_x^2 - \gamma^2}}{2\xi^3}. \tag{9}$$

Having determined that ground states can be formed in a storage ring with AG (time-dependent) focusing, we studied the effect of shear upon the ground state: i.e., the effect of time varying bending. We took an AG lattice of the FODO-type which has the similar transverse tunes as the previous constant-bending case, but with the bending concentrated into a small region (25%) of the lattice period. Fig. 2 shows a crystal formed in such a machine. The typical particle trajectories within one machine period are shown in Fig. 3. It can be seen that the crystal "takes up the difference" between constant angular velocity and constant linear velocity

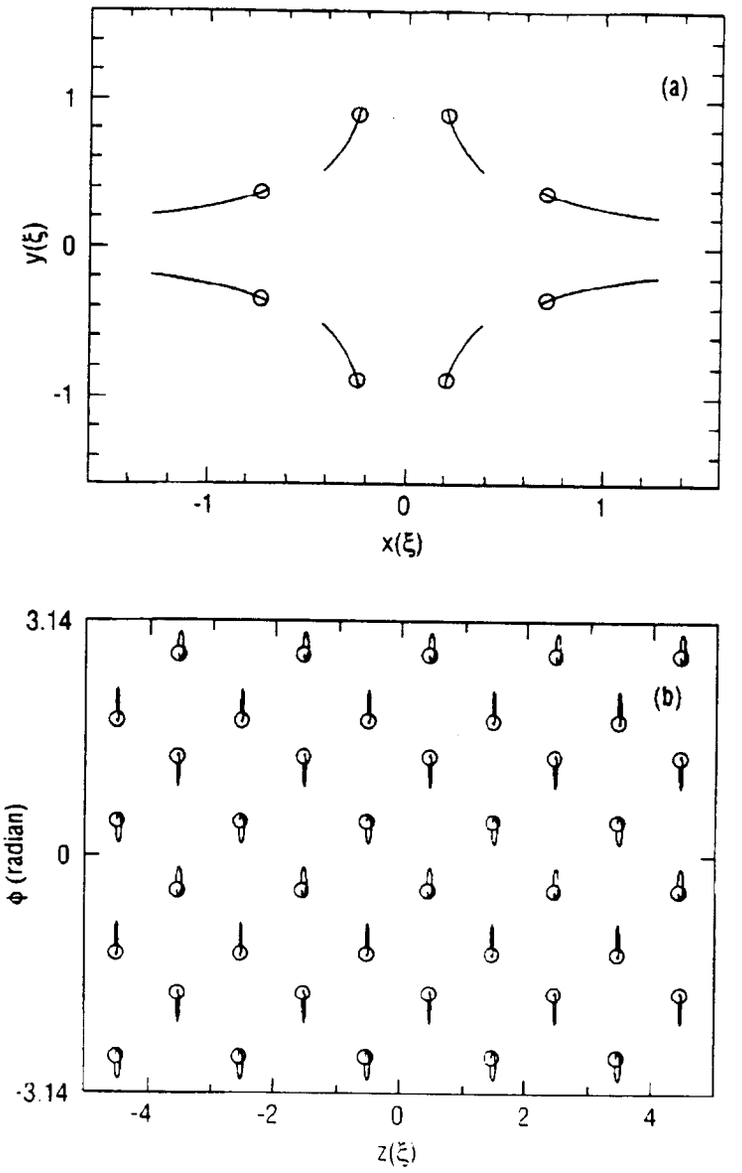

Figure 1: A single-shell structure with particle positions projected (a) into the $x-y$ plane and (b) into the $\phi - z$ plane, where ϕ is the polar angle. The machine consists of 10 FODO (focusing, open or drift, defocusing, open or drift) cells with constant bending with $\nu_x = 2.7$ and $\nu_y = 2.3$, and the particle energy is $\gamma = 1.4$. The number of particles (N) per MD super-cell is 40 and the MD super-cell length (L) is 10ξ. The particles move periodically in time, with the solid lines showing their trajectories and the circles indicating their positions at the start and end of each lattice period.

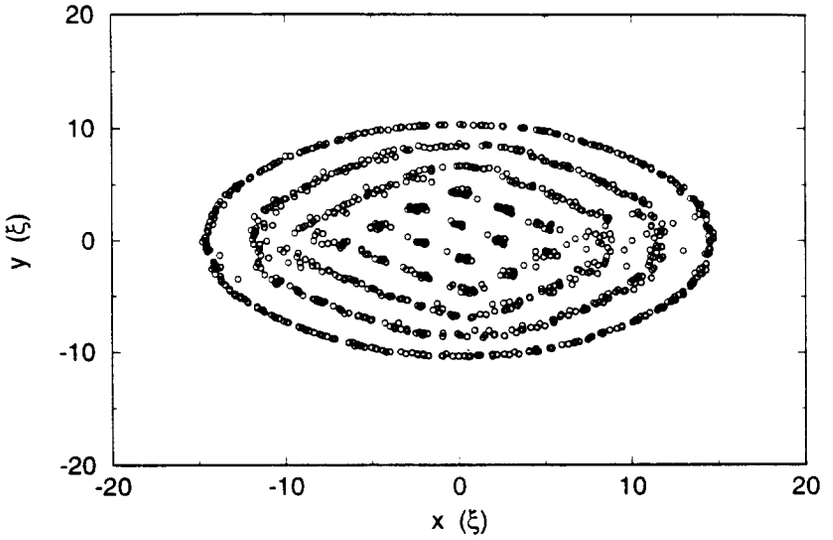

Figure 2: A multi-shell structure with particle positions projected into the $x-y$ plane. The machine consists of 10 FODO cells with 25% bending with $\nu_x = 2.8$, $\nu_y = 2.1$, and the particle energy is $\gamma = 1.4$. The calculation is done with $N = 1000$ and $L = 40\xi$.

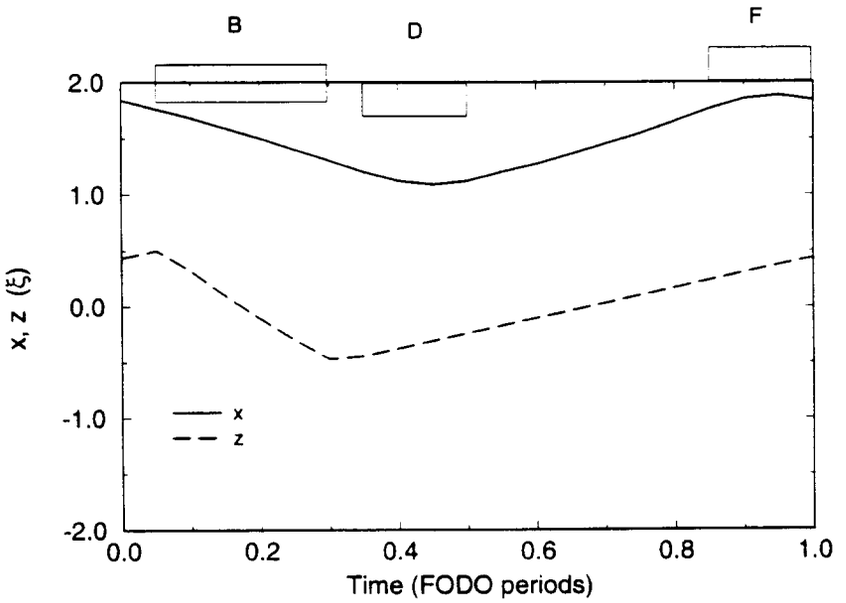

Figure 3: The effect of shear. In this study $N = 40$, $L = 40\xi$. Motion occurs both in the x direction (breathing) and in the z direction (shear) for a particle (with largest horizontal displacement and no vertical displacement) through a lattice cell. Lattice components are displayed on the figure, B is a bending section, F is a focusing section, D is a defocusing section. The machine parameters are the same as that used in Fig. 2, with $\gamma = 1.4$, $\nu_x = 2.8$ and $\nu_y = 2.1$.

by adjusting the spacing between particles; i.e., by converting potential energy into kinetic energy.

A more extreme case is supplied by the Heidelberg TSR lattice,[27] which has a periodicity of 2 and rather sharp bends in each of the corners. We have taken the case where the number of particles per super-cell, $N = 20$, and where the super-cell length, $L = 100\xi$, and find a 2-D crystalline state (zig-zag) which has the symmetry of the lattice and numerically appears to be stable. The state makes one rotation per lattice period around its longitudinal axis, having a horizontal orientation in the middle of the straight sections with particle separation of 2.5ξ, and a vertical orientation in the middle of the bending region with particle separation 8.7ξ! The rotation is produced by the shear motion when the particle crosses the bending magnetic field and is shown in Fig. 4. The direction of the rotation is determined by the orientation of the bending magnetic field.

6. CORRELATION FUNCTIONS AND BREAK-UP TEMPERATURE

Having studied the crystalline-beam ground state, we investigated behavior at non-zero temperatures.[20] – [22] For this time-dependent Hamiltonian system, we define the temperature in terms of the deviation of P_x, P_y and P_z from their ground-state values,

$$T_x = \langle (\Delta P_x)^2 \rangle, \quad T_y = \langle (\Delta P_y)^2 \rangle, \quad \text{and} \quad T_z = \langle (\Delta P_z)^2 \rangle, \tag{10}$$

squared and averaged both over different particles and over a time period (typically 20 lattice periods) that is long compared with the focusing period but short compared with the total time of observation. The temperature can readily be expressed in terms of the usual accelerator parameters of un-normalized emittances, ϵ_x and ϵ_y, and relative momentum spread, $\Delta p/p$, by

$$\left(\Delta\epsilon_x, \Delta\epsilon_y, \frac{\Delta p}{p} \right) = \left(\frac{\xi^2}{\rho^2}\bar{\beta}_x T_x, \frac{\xi^2}{\rho^2}\bar{\beta}_y T_y, \frac{\xi}{\rho}\gamma\sqrt{T_z} \right). \tag{11}$$

The systems we study are all one-dimensional in the sense that in the two directions perpendicular to the beam, the systems are always finite. Two qualitatively different states exist in these systems, one is a low temperature "condensed state" (crystalline beam), in which there is limited shearing motion in the z direction, but no passing of particles, and the other is a high temperature "running state" in which particles shear, in an un-limited manner, relative to each other. The temperature T_z at which the transition occurs is called the break-up temperature.

The distinction between the running and the condensed states can be found in the ordering in azimuthal direction, which is characterized by the two-body correlation function $G_2(z)$

$$G_2(z) = \left\langle \frac{1}{N^2} \sum_{i,j=1, i\neq j}^{N} \delta\left(z - |z_i - z_j|^N\right) \right\rangle_t \tag{12}$$

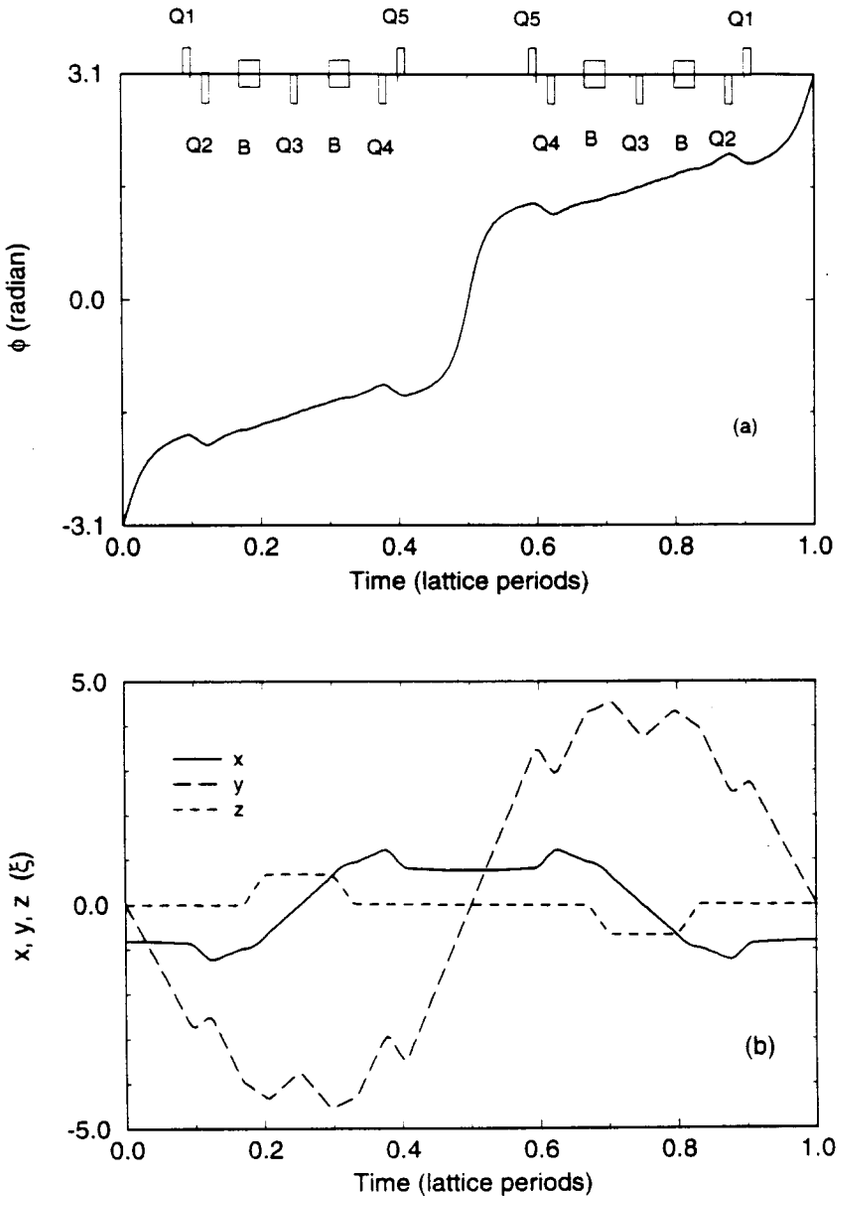

Figure 4: A zig-zag structure formed with the Heidelberg TSR machine lattice with (a) the polar angle ϕ and (b) displacements in x, y, and z of the particle changing with time during one lattice period. Lattice components are displayed on the figure. and the lattice periodicity is 2.

where $\langle\ \rangle|_t$ denotes the average over time after thermal equilibrium is reached. As the temperature increases, the beam transforms from the condensed, ordered state in z into the running state. Similarly, the ordering in transverse direction can be described by the time-averaged density distribution functions. For a 3-D structure, computer results indicate that as the temperature increases, the beam becomes disordered first transversely in ϕ and ρ, and then longitudinally in z (as shown later in Fig. 8).

The break-up temperature depends upon both the machine parameters and the beam density. The dash line in Fig. 5a indicates the break-up temperature for a

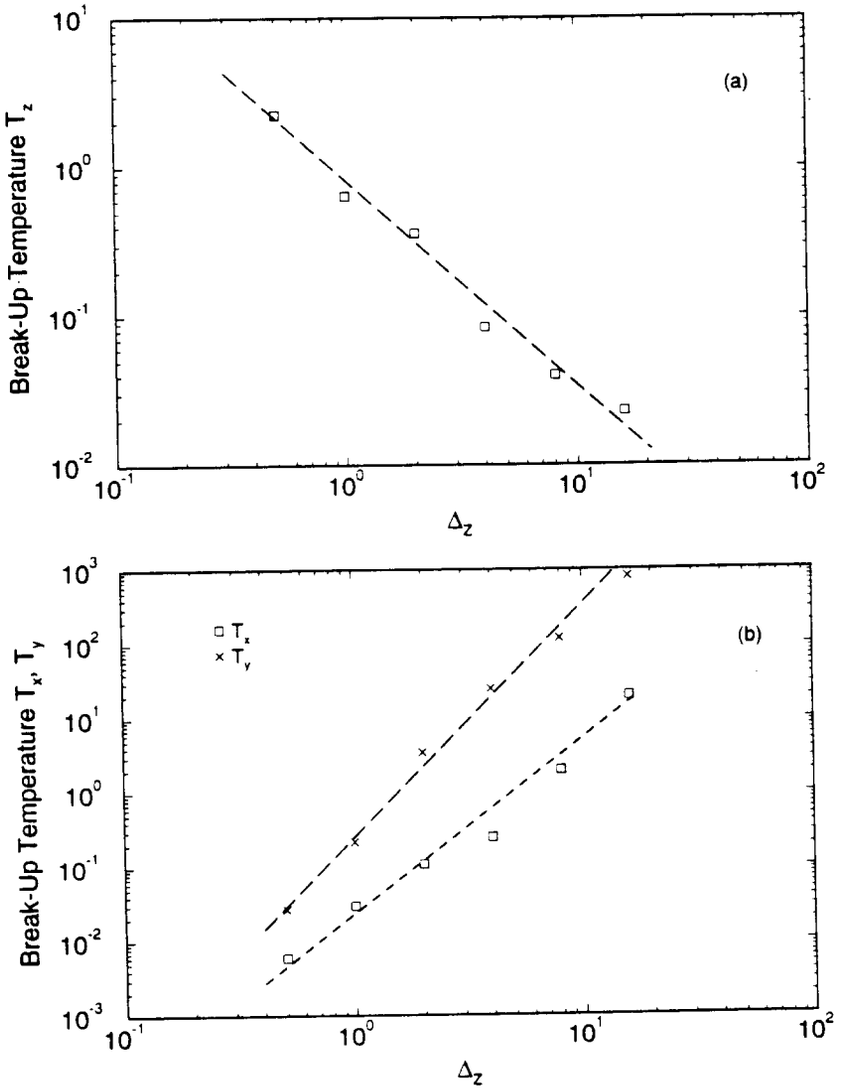

Figure 5: Break-up temperatures in the (a) azimuthal and (b) transverse direction as functions of the inverse of the beam density. The machine parameters are the same as that in Fig. 1. The result has been verified by comparing cases with different L and N (N =10, 20, 50, 100, and 200) while keeping the line density $\Delta_z^{-1} = N/L$ constant ($\Delta_z = 2$).

constant-bending AG machine obtained by perturbing the particles from their crys-

talline ground-state position in the azimuthal direction z only. The approximate relation

$$T_z \approx 0.6\ \Delta_z^{-1} \tag{13}$$

implies that the break-up in azimuthal direction occurs when the average kinetic energy is comparable to the potential energy difference needed for part of the particles to traverse a significant fraction of the distance Δ_z. When T_z is lower than this temperature, particles vibrate azimuthally around their ground-state positions. Almost no thermal energy is transferred into the y direction, and very little is transferred into the x direction (due to x-z coupling). When T_z is above this temperature, thermal energy in z is rapidly transferred into transverse directions, and the crystal melts at the same time.

Fig. 5b corresponds to the cases when the beam is perturbed from their ground-state values transversely in either the x or y direction, but not in the z direction. The dashed lines corresponds to the values when the beam breaks up in the z direction. The beam break-up occurs when the transverse vibrational displacement is comparable to the ground-state interparticle distance. Since the vibrational frequencies in transverse directions are mainly determined by the external transverse focusing (Eq. 15), the break-up temperatures $T_{x,y}$ are approximately proportional to Δ_z^2. The fact that T_x is lower than T_y is partly due to the coupling between the x and z motion. Note the completely different dependence of T_z and the transverse temperatures, T_x and T_y, upon density Δ_z^{-1}.

Consider the constant-bending storage ring example, discussed previously, with $2\pi R$ =24 m and $\bar{\beta}_{x,y} \approx 10$ m. ξ is equal to 1.8 μm for proton, and is equal to 22 μm for electron. The condition to form a crystalline beam can be expressed using Eq. 11 as

$$\left(\Delta\epsilon_x, \Delta\epsilon_y, \frac{\Delta p}{p}\right) < \begin{cases} \left(0.8\times 10^{-11}T_x, 0.9\times 10^{-11}T_y, 1.3\times 10^{-6}\sqrt{T_z}\right) & \text{(proton)} \\ \left(1.2\times 10^{-9}T_x, 1.3\times 10^{-9}T_y, 2.1\times 10^{-5}\sqrt{T_z}\right) & \text{(electron)} \end{cases} \tag{14}$$

where the break-up temperatures T_x, T_y, and $\sqrt{T_z}$ are given by Fig. 5.

7. MECHANISM FOR HEAT TRANSFER

Since a constant gradient storage ring can not have a crystalline beam, the Hamiltonian is necessarily time-dependent, and the total energy of the system is not a constant of the motion. Furthermore, the Hamiltonian, without the smooth approximation, is not bounded from below at any time and the adiabatic approximation can not be used. It is precisely the dynamical coupling between the external focusing-defocusing force and the Coulomb interaction among the particles that gives us the well-defined periodic structures which we call the "ground state". However, the time dependence of the Hamiltonian can cause damage to the crystal, because energy can be pumped into the system by creating phonons. As a result, a crystalline beam at non-zero temperatures can not last forever unless energy is pumped out of the system

by means of a refrigerator. Here, we answer the question how fast heat transfers into the system, and derive yet another criterion that has to be satisfied for high-quality crystalline beams to exist.[22]

In the limit of smooth approximation, the Hamiltonian is time-independent, and it is trivial to calculate the phonon spectrum. Take a 1-D chain as an example, the three branches of dispersion are,

$$\begin{aligned} \omega_{1,3}^2(k) &= \frac{1}{2}\left\{\nu_x^2+\Omega_k^2 \pm \left[(\nu_x^2+\Omega_k^2)^2 - 8\Omega_k^2(\nu_x^2-\gamma^2-\Omega_k^2)\right]\right\}^{\frac{1}{2}}, \\ \omega_2^2(k) &= \nu_y^2-\Omega_k^2, \end{aligned} \tag{15}$$

where

$$\Omega_k^2 = 2\sum_{n=1}^{\infty}\frac{1-\cos(kn\Delta_z)}{n^3\Delta_z^3}, \tag{16}$$

the crystal momentum k is between $-\pi/\Delta_z$ and $+\pi/\Delta_z$, and Δ_z is the interparticle distance. Since the y direction is not coupled with the x and z directions, ω_2 is purely polarized in the y direction. The x and z directions are coupled with each other, but at $k=0$, $\omega_1=\nu_x$ (with the plus sign) is purely x polarized, and $\omega_3=0$ (with the minus sign) is purely z polarized. The phonon modes are singular at $k=0$ due to the long range Coulomb interaction, but the singularity is very week, only logarithmic in nature (actually $k[\log(k)]^{1/2}$), and does not cause any qualitative difference in the properties of the crystalline beams. Typical density of states (DOS) is shown in Fig. 6a. The highest phonon frequency, ω_m, is in many cases (although not always) the larger of ν_x and ν_y. Under certain conditions, $\omega_1(k)$ can be larger than ν_x, but only marginally so.

At higher density, the ground state structure becomes two- or three-dimensional, and the phonon modes can no longer be found analytically, but must be calculated numerically. It is found that the phonon frequencies can go from zero to ω_m continuously, the weak singularity at $k=0$ is still there, and it is still true that the highest phonon frequency ω_m is closely related to the larger of ν_x and ν_y.

Beyond the smooth approximation, time-dependent terms like $\cos(\omega_l t)x^2$ and $\cos(\omega_l t)y^2$ appear in the Hamiltonian, where ω_l is the AG lattice frequency. Since x and y vibrate with the phonon frequencies $\omega_{1,2,3}(k)$, these time-dependent terms generate vibrations with frequencies $\omega_l \pm \omega(k)$, as shown in Fig. 6b. These frequencies form a band between $\omega_l-\omega_m$ and $\omega_l+\omega_m$, and the band is generally continuous except at very low density. Typically, a series of continuous bands between $j\omega_l-\omega_m$ and $j\omega_l+\omega_m$ will form, where j is an integer, due to the higher component in the Fourier expansion of focusing-defocusing forces in the AG lattice.

If the AG lattice frequency ω_l is smaller than twice the maximum phonon frequency ω_m, then the phonon band between 0 and ω_m overlaps with the vibrational band between $\omega_l-\omega_m$ and $\omega_l+\omega_m$, and resonance occurs, and the vibrational amplitude of the particles grows exponentially, and the crystalline beam will be instantly destroyed. Therefore, in order for the crystalline beam to last a meaningful length of time, ω_l has to be larger than $2\omega_m$, i.e., the storage ring should be designed such that the lattice periodicity is at least twice as high as the betatron frequency.

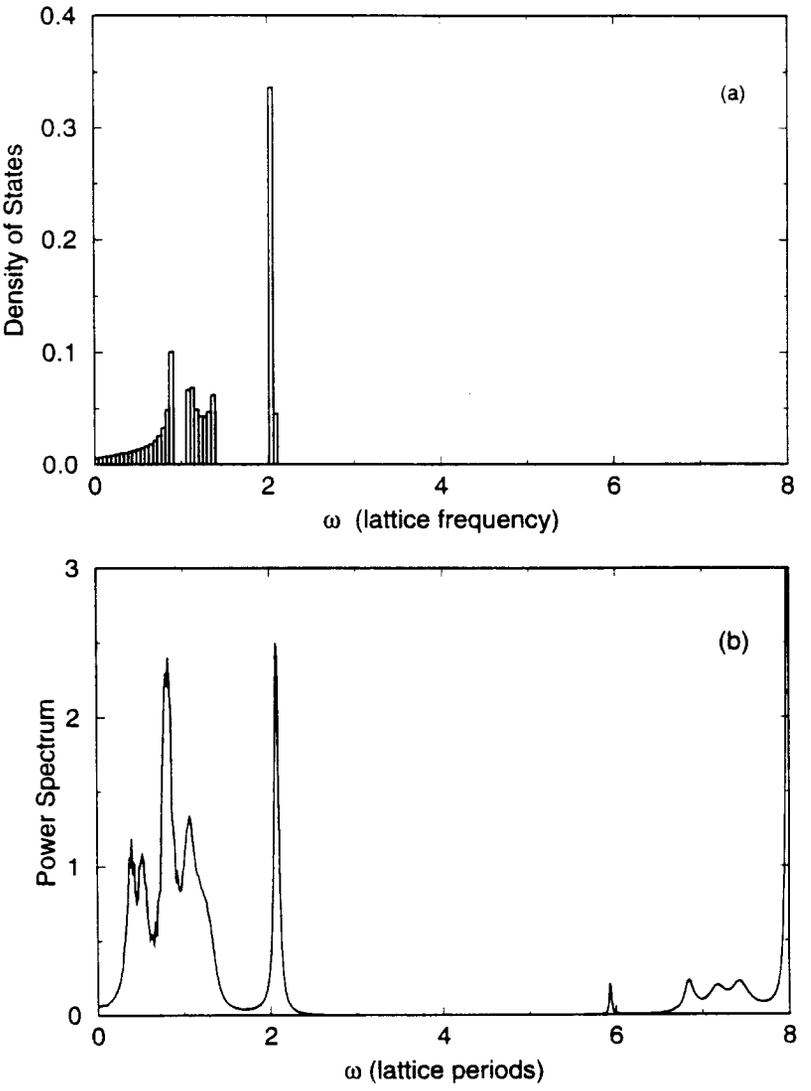

Figure 6: Vibrational density of states (a) under smooth approximation and (b) for the exact Hamiltonian from molecular dynamics (with $N = 100$ and $L = 180\xi$) for a 1-D chain. The machine consists of 8 lattice periods, each containing a FODO cell and an insertion (containing drift spaces and two quadrupole magnets), with $\nu_x = 2.07$, $\nu_y = 1.38$, and $\gamma = 1.1$.

With the shear lattice example discussed previously in Figs. 2 and 3, the machine lattice periodicity (10) is much higher than the highest phonon frequency ($\nu_x = 2.8$) in the system. The transfer of energy into the system can only be realized by multi-phonon emission. This process is expected to be strongly temperature-dependent. We have studied the relation between the heating rate and the temperature. Fig. 7 shows the survival time (time before particles slip past each other, or crystal break-up) of a crystalline beam without cooling as a function of the initial temperature at which a MD run starts. The survival time indeed strongly depends on the initial temperature, and rapidly tends to a large value when the initial temperature is low enough. This indicates that at low temperature, the rate that energy transfers into the system is very low, and it is easy to maintain a crystalline beam for a long time. Fig. 8 shows the heat transfer rate as a function of the temperature. As the temperature increases, the single-shelled crystalline beam (phase I) appears to first become disordered in the transverse direction (ϕ) (phase II). As the temperature increases beyond the break-up value, $T \approx 0.3$, the beam then becomes disordered azimuthally (phase III). Fig. 9 a–d show the correlation functions $G_2(z)$ for a variety of temperatures.

8. CONCLUSIONS AND DISCUSSION

In this report, we have attempted to cover the present state of knowledge concerning crystalline beams. First reviewing what we have presented we shall, then, discuss some of the remaining subjects which might be studied theoretically. Of course, the primary subject must be the experimental realization of a crystalline beam, and we know that there are at least two groups actively trying to do just that. Their experimental work requires an ever-better understanding of the sources of heat, and an ever-more effective cooling methods.

In summary, then, we introduced the Hamiltonian (Section 2) describing the self interaction of a group of particles, subject also to external forces, in the rotating beam frame. This frame proved convenient for adopting the methods of molecular dynamics (Section 4). Prior to using numerical methods we were able to establish (Section 3) that crystals can only be formed in AG-focusing rings operated below the transition energy.

We first turned our attention to ground state structures (Section 5) and found that depending upon machine parameters and particle density, they consisted of 1-D, 2-D, or 3-D structures. These structures are similar to the pioneering work done in harmonic wells, but they differ in detail. We found that these structures can be formed no matter how varied the ring is (high shear and AG focusing) and no matter how high is the particle density.

We then turned our attention to finite-temperature effects (Section 6), and found that above certain transverse and longitudinal temperatures, called the "break-up temperatures", which are given in terms of the usual accelerator parameters of energy spread and emittance, a crystal melts: i.e., particles slip past each other. Increasing the temperature from zero, we found that one reaches a lower temperature than the break-up temperature where, suddenly, the crystal is very effective in picking up heat

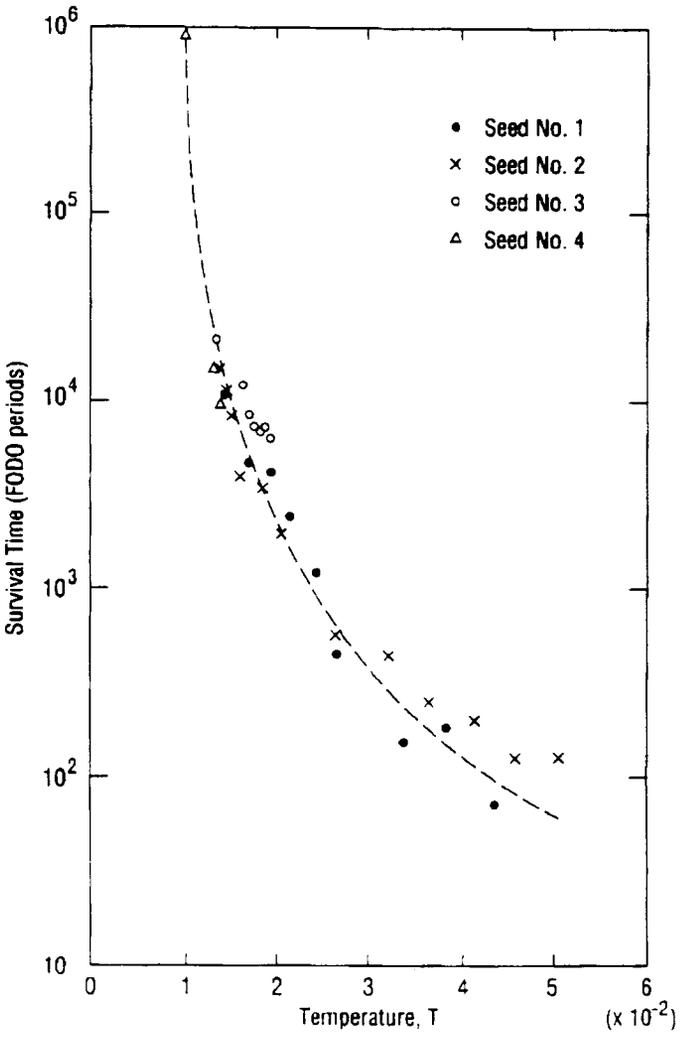

Figure 7: A study of survival time of a crystal, in the absence of cooling, as a function of the initial temperature of the crystal. For these studies the same lattice and beam parameters were employed as in Fig. 3. In all cases $N = 40$ and $L = 40\xi$. More than one point, at the same temperature, is due to different random seeds used to distribute initial particle position and velocity appropriate to the chosen temperature.

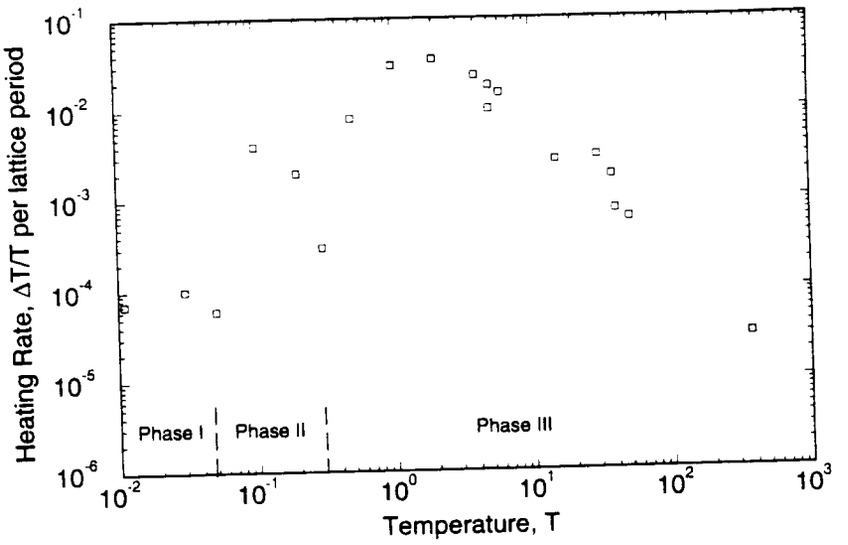

Figure 8: The heating rate as a function of the temperature T. The machine and beam parameters are the same as that used in Fig. 7. The break-up temperature is about $T \approx 0.3$.

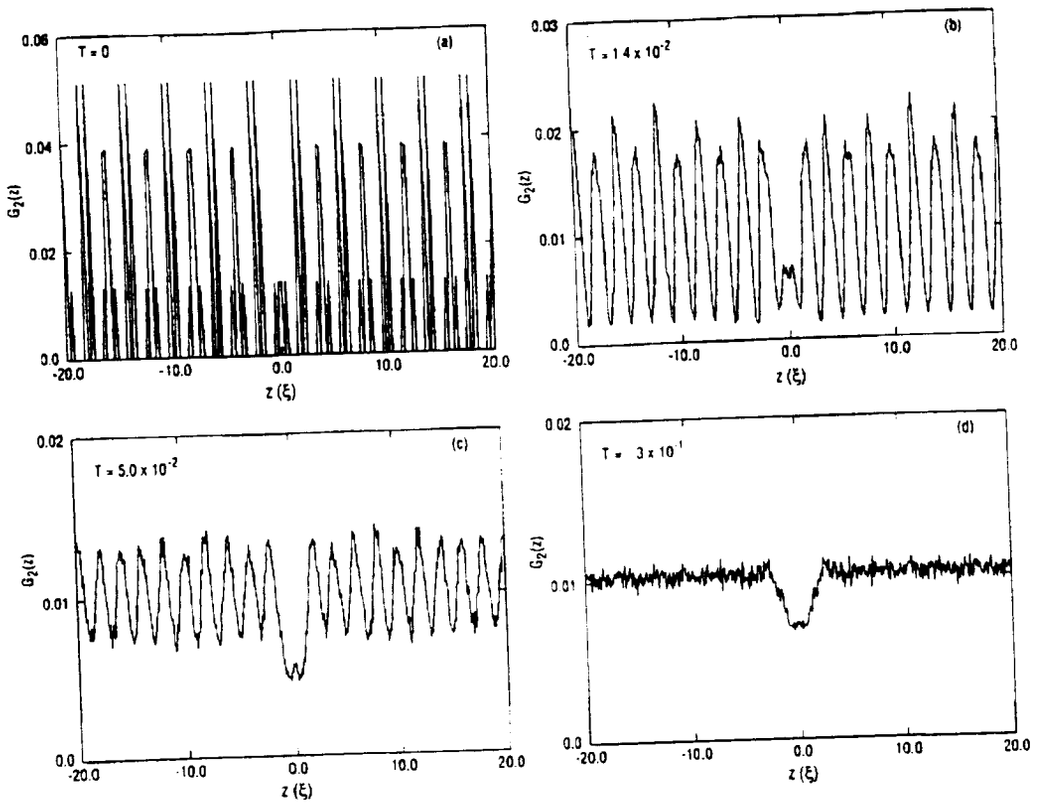

Figure 9: Two-body correlation function $G_2(z)$ at various temperatures. The machine and beam parameters are the same as that used in Fig. 7.

from the lattice. The mechanism for this (Section 7) is that two phonon excitation has become possible. The criterion that this not occur, which becomes the second necessary criterion for the formation of crystals, is that the lattice periodicity must be at least twice the betatron frequency.

Although a great deal has been done on crystalline beams, there is still a great deal more to do. Some of the things to be done are relatively straightforward, that is, they involve the use of techniques that are established, but not yet employed; other calculations require novel approaches.

As an example of a rather straightforward calculation, we can think of the task of developing the heating curve for the ASTRID lattice; or checking that the heating curve goes over, at high temperatures, into the (well-known) multiple scattering theory for particle beams; or developing the heating curve for various values of the ratio of perpendicular temperature to longitudinal temperature; or studying of the crystals in the ASTRID lattice with ν_x and ν_y both less than two (so as to satisfy the second criterion for crystal formation). Here one needs to determine the 1-D, 2-D, 3-D structures and also determine the heating curve. Also in this category of relatively straightforward things is a careful study of the order of the transition between 1-D, 2-D, and 3-D shapes.

Also straightforward, would be a study of the theoretical expectations for the old experiment, from which it all started, on NAP-M.[28] The theory is now in a position to do this calculation, and it would be most interesting to know if the experimental observations are in accord with current theory.

Another area that might be studied theoretically is on crystals under the influence of RF field such as might be convenient for limiting the crystal in azimuth or facilitating laser cooling.[29]

Careful study needs to be made of the effect of machine errors. A start along this direction has been made by two different groups, with two different answers, so the subject is in need of definitive work.

It would be very useful for the experimentalists if the theorist were to calculate the expected Schottky signals on beam pick-ups. (This is relevant to the NAP-M experience, but it is more general.) A theory of the expected signals at high temperatures has been developed by V. Lebedev.[30] (This theory is for lower temperatures than that of the usual single particle noise theory, but higher temperatures than that associated with crystal formation.) The evaluation of expected Schottky signals should go over into Lebedev's theory as a crystal melts.

There are a number of theoretical topics that are not so straightforward. One is to develop a theory of the heating curve (at least for the peak value and width of peak). This would allow one to see the dependence upon lattice, shear and AG focusing, transverse and longitudinal temperature, etc. A second subject might be to understand the role of very low phonon k values and, in particular, to understand the cascade of energy to ever-lower frequencies, as described by R.W. Hasse.[8] A third subject might be to study crystals of many species.

In sum, then, the subject of crystalline beams has already stimulated much theoretical work and much experimental effort. It promises to be even more interesting in future years.

We want to acknowledge the assistance of R.W. Hasse in making our computer program more efficient. We had useful conversations with J.S. Hangst, D. Habs, J.P. Schiffer, V.J. Emery, I. Hofmann, and V.V. Avilov.

9. REFERENCES

1. J.P. Schiffer and P. Kienle, Z. Phys. A **321**, 181 (1985).
2. J.P. Schiffer and O. Poulsen, Europhys. Lett. **1**, 55 (1986).
3. A. Rahman and J.P. Schiffer, Phys. Rev. Lett. **57**, 1133 (1986).
4. D. Habs, MPI Heidelberg preprint MPIH-1987-V10 (1987).
5. J.P. Schiffer, Phys. Rev. Lett. **61**, 1843 (1988).
6. R.W. Hasse and J.P. Schiffer, Ann. Phys. **203**, 419 (1990).
7. R.W. Hasse, GSI preprint GSI-90-23 (1990).
8. R.W. Hasse and V.V. Avilov, Phys. Rev. A **44**, 4506 (1991).
9. J.P. Schiffer, Phys. Rev. Lett. **70**, 818 (1993).
10. J.P. Schiffer and A. Rahman, Z. Phys.A - Atomic Nuclei 331, 71–74 (1988).
11. J.P. Schiffer, Proceedings of the Workshop on Crystalline Ion Beams, Werheim, Germany, 2 (1988), ed. R.W. Hasse, I. Hofmann, D. Liesen.
12. J.P. Schiffer and A. Rahman, Z. Phys.A-Atomic Nuclei **331**, 71 (1988).
13. J.P. Schiffer, Proc. of the Workshop on Crystalline Ion Beams, Werheim, Germany, editors R.W. Hasse, I. Hofmann, and D. Liesen, p.2 (1988).
14. *CRYSTAL -A Storage Ring for Ion Beam Crystallisation Studies*, LNL-INFN (REP) 59/92, Laboratori Nazional di Legnaro.
15. J. Beebe-Wang, N. Elander and R. Schuch, Nucl. Instrum. Methods **B79**, 806 (1993).
16. S. Schroder et al, Phys. Rev. Lett. **64**, 2901 (1990).
17. J.S. Hangst, et al, Phys. Rev. Lett. **67**, 1238 (1991).
18. J. Wei, X-P Li, and A.M. Sessler, "Crystalline Beam Ground State", Brookhaven National Laboratory Report BNL-52381, Upton, New York (1993).
19. J. Wei, X-P Li, and A.M. Sessler, "Crystalline Beam Ground State", Proc. of The 1993 Particle Accelerator Conference,Washington, May 1993, p. 3527.
20. J. Wei, X-P Li, and A.M. Sessler, "Critical Temperatures for Crystalline Beams", Proc. of the Workshop on Beam Cooling and Related Topics, Montreux, October 1993, p. 366.
21. J. Wei, X-P Li, and A.M. Sessler, "The Low-Energy States of Circulating Stored Ion Beams: Crystalline Beams", submitted to Physical Review Letters (March 1994).

22. X-P Li, A.M. Sessler, and J. Wei, "Crystalline Beams in a Storage Ring: How Long Can It Last", Proc. of the 1994 European Particle Accelerator Conference, London, June 1994 (to be published).

23. C. Møller, *The Theory of Relativity*, Oxford, 1952.

24. P.P. Ewald, Ann. Phys. (Leipzig) **64**, 253 (1921).

25. V.V. Avilov, Solid State Comm. **44**, 555 (1982).

26. R.W. Hasse, Phys. Rev. Lett. **67**, 600 (1991).

27. D. Habs-private communication.

28. E.E. Dement'ev, N.S. Dikanskiĭ, A.S. Medvedko, V.V. Parkhomchuk and D.V. Pestrikov, Zh. Tekh. Fiz **50**, 1717 (1980); English transl. Sov. Phys. Tech. Phys. **50**, 1001 (1980).

29. H. Okamoto, D. Möhl, and A.M. Sessler, Phys. Rev. Lett. **72**, 3977 (1994).

30. V. Lebedev, Presentation at the Discussion Meeting on Cold Stored Ion Beams, Heidelberg, July 1994.

APPENDIX

In order to obtain the condition for crystallization, we first eliminate the cross term in the Hamiltonian Eq. 3 by using a canonical transformation

$$F_2(x, \bar{P}_x, y, \bar{P}_y, z, \bar{P}_z) = (x - \gamma D \bar{P}_z)(\bar{P}_x + \gamma D' \bar{P}_z) + y\bar{P}_y + z\bar{P}_z, \qquad \text{(A-1)}$$

where the function D is determined by eliminating the cross terms in the Hamiltonian at both the bending (Eq. 3) and the straight sections (Eq. 5), i.e.

$$D'' + K_x D = \begin{cases} 1 & \text{(bending section)} \\ 0 & \text{(straight section).} \end{cases} \qquad \text{(A-2)}$$

Obviously, D thus defined is the horizontal dispersion of the machine normalized by the bending radius ρ. With Eq. A-1, the new Hamiltonian becomes

$$\bar{H} = H + \frac{\partial F_2}{\partial t} = \frac{1}{2}\left(\bar{P}_x^2 + \bar{P}_y^2\right) + \frac{1 - \gamma^2 F_z}{2}\bar{P}_z^2 + \bar{V}_C, \qquad \text{(A-3)}$$

where the Coulomb potential $\bar{V}_C$ is given by V_C with the variables x, y, and z substituted by the new variables $\bar{x}$, $\bar{y}$, and $\bar{z}$, and

$$F_z = \begin{cases} D + DD'' + (D')^2 & \text{(bending section)} \\ DD'' + (D')^2 & \text{(straight section).} \end{cases} \qquad \text{(A-4)}$$

The average value of F_z can be obtained as

$$\langle F_z \rangle = \frac{\rho}{2\pi R}\oint F_z dt = \frac{\rho}{2\pi R}\oint_{\text{bend}} D dt \equiv \frac{1}{\gamma_t^2}, \qquad \text{(A-5)}$$

where γ_t is the transition energy of the machine. Using the generating function F_2 (Eq. A-1), the new variables are related to the old ones by the equations

$$\begin{cases} \bar{x} &= x - \gamma D \bar{P}_z \\ \bar{y} &= y \\ \bar{z} &= z + \gamma D' x - \gamma D \bar{P}_x - 2\gamma^2 D D' \bar{P}_z, \end{cases} \tag{A-6}$$

and

$$\begin{cases} P_x &= \bar{P}_x + \gamma D' \bar{P}_z \\ P_y &= \bar{P}_y \\ P_z &= \bar{P}_z. \end{cases} \tag{A-7}$$

The Hamiltonian (Eq. A-3) can be further simplified by expressing it in terms of the conventionally defined action-angle variables

$$\bar{H} = \nu_x J_x + \nu_y J_y + \frac{1 - \gamma^2 F_z}{2} \bar{P}_z^2 + \bar{V}_C, \tag{A-8}$$

where J_x and J_y are the actions, and the transverse tunes ν_x and ν_y are positive for a stable machine lattice.

For a stable crystalline beam, the Coulomb force must on the average provide focusing in the azimuthal direction,

$$\bar{V}_C \approx \frac{k_z}{2} \bar{z}^2, \quad \text{for } \bar{z} \ll \Delta_z, \tag{A-9}$$

where $k_z \geq 0$ is the effective Coulomb focusing strength. It can thus be seen from Eqs. A-8 and A-5 that the azimuthal motion will not be bounded if $\gamma \geq \gamma_t$. Hence, the crystalline beam can not form when the beam energy γ is above the transition energy γ_t.

On the other hand, for a cyclotron magnet, $D = K_x^{-1}$, $F_z = D$, and $K_x = 1 - n$, so one obtains the condition for positive definiteness of $\bar{H}$ (Eq. A-8) that $1 - \gamma^2 > n$, which can never be satisfied.